International Journal of Nanomedicine Dovepress

Open Access Full Text Article ORIGINAL RESEARCH

Nebulization of Hypoxic hUCMSC-EVs Attenuates Airway Epithelial Barrier Defects in Chronic Asthma Mice by Transferring CAV-1

Xinkai Luo[1,*], Ying Wang[2,*], Yufei Mao[3,*], Xiaowei Xu[1,4], Weifeng Gu[1], Wen Li[1], Chaoming Mao[1], Tingting Zheng[1], Liyang Dong[1]

[1]Department of Nuclear Medicine, The Affiliated Hospital of Jiangsu University, Zhenjiang, Jiangsu, People's Republic of China; [2]Department of Respiratory Diseases, The Affiliated Huai'an Hospital of Xuzhou Medical University, Huai'an, Jiangsu, People's Republic of China; [3]Department of Ultrasound Medicine, The Affiliated Hospital of Jiangsu University, Zhenjiang, Jiangsu, People's Republic of China; [4]Department of Laboratory Medicine, The Affiliated Suzhou Hospital of Nanjing Medical University, Suzhou, Jiangsu, People's Republic of China

*These authors contributed equally to this work

Correspondence: Liyang Dong; Tingting Zheng, Email liyangdong@ujs.edu.cn; tingtingzheng@ujs.edu.cn

Background: Nebulization of hypoxic human umbilical cord mesenchymal stem cell-derived extracellular vesicles (Hypo-EVs) can suppress airway inflammation and remodeling in a chronic asthmatic mouse; however, the exact mechanism remains unclear. Recently, airway epithelial barrier defects have been regarded as crucial therapeutic targets in asthma. The aim of this study was to investigate whether and how Hypo-EVs protect against the disruption of the airway epithelial barrier under asthmatic conditions.

Methods: The therapeutic effects of Hypo-EVs on airway epithelial barrier defects were evaluated in ovalbumin (OVA)-induced asthmatic mice and in IL-4 and IL-13-induced HBE135-E6E7 cell models by detecting cell monolayer leakage and junctional protein expression. The protein levels in Hypo-EVs were determined by Western blotting, and a gene knockdown approach was used to investigate the biofactors in Hypo-EVs.

Results: Nebulization of Hypo-EVs directly alleviated airway epithelial barrier defects in asthmatic mice, as evidenced by colocalization with bronchial epithelial cells, decreased albumin concentration, and increased ZO-1 and E-cadherin expression. In vitro, Hypo-EV treatment dramatically rescued the increase in airway cell permeability, and upregulated the ZO-1 and E-cadherin protein expressions. Based on WB analysis, we found that caveolin-1 (CAV-1) was strongly enriched in Hypo-EVs. The knockdown of CAV-1 protein levels in Hypo-EVs significantly impaired Hypo-EV-mediated barrier protection in vitro and in vivo. Moreover, CAV-1 knockdown significantly abolished the beneficial effects of Hypo-EVs on airway inflammation and remodeling in asthmatic mice. In addition, we showed that IL-4/IL-13-induced airway epithelial barrier defects were mainly related to activation of STAT6 phosphorylation (p-STAT6), and overexpression of CAV-1 or Hypo-EV treatment inhibited the levels of p-STAT6 in IL-4/IL-13-induced HBE135-E6E7 cells.

Conclusion: Nebulization of Hypo-EVs can attenuate airway epithelial barrier defects in asthma by delivering CAV-1 to inhibit p-STAT6 expression and may be used to treat other barrier defect diseases.

Keywords: nebulization, Hypo-EVs, asthma, airway epithelial barrier, caveolin-1

Introduction

Asthma is a common chronic respiratory disease that affects at least 300 million people worldwide.[1] It is characterized by airway inflammation and remodeling, which may result in small airway narrowing, exhalation dysfunction and even patient death.[2] Inhaled corticosteroids are the most basic treatment for asthma; they can provisionally control respiratory symptoms but do not focus on disease regression, additionally, their long-term use has certain side effects on general health.[3,4] Therefore, effective and safe therapeutic strategies for asthma are urgently needed.

Received: 29 April 2024
Accepted: 19 October 2024
Published: 29 October 2024

The pathogenesis of asthma has been the subject of intensive study in recent decades, and it is now widely accepted that the disruption of airway epithelial barrier (AEB) represents a key factor in the aetiology of asthma.[5,6] The AEB is constituted by adjacent bronchial epithelial cells, with junctional proteins (such as E-cadherin and ZO-1) attaching to neighbouring cells and controlling paracellular transport. In asthmatic conditions, the AEB function is impaired, as indicated by decreased junctional protein expression and increased epithelial barrier permeability, which enables external allergens to penetrate the airway submucosa, subsequently triggering the type-2 inflammation response.[7] Type-2 immune cytokines, such as interleukin-4 (IL-4) and IL-13 induce a number of processes associated with the development of airway inflammation and remodeling, including eosinophil recruitment, goblet cell hyperplasia, and extracellular matrix deposition. In addition, these cytokines have also been demonstrated to diminish the expression of junctional proteins, thereby further increasing epithelial barrier permeability.[8,9] Clearly, protecting AEB function is a rational approach to attenuate asthma.[10]

Extracellular vesicles (EVs) are double-layered lipid nanoscale vesicles secreted by almost all cell types. In recent years, EVs, especially those derived from mesenchymal stem cells (MSC-EVs), have been considered an extremely promising cell-free therapeutic agent, as they circumvent the risks of tumourgenicity, immune rejection, and ethical issues inherent to MSC therapy.[11,12] To date, accumulating evidence has shown that exogenous MSC-EVs have anti-inflammatory properties in several stabilized asthma murine models.[13] However, the protective effect of MSC-EVs on the AEB during asthma remains unclear.

We previously reported that a hypoxic environment could promote human umbilical cord MSCs (hUCMSCs) to release more EVs, which we termed Hypo-EVs.[14] Recently we revealed that these EVs can be administered by atomization, and nebulization of Hypo-EVs not only effectively inhibited allergic airway inflammation, but also showed excellent biological safety in a mouse model, which provides a promising noninvasive MSC-EV-based treatment approach for asthma disease.[15] In the present study, we further investigated the effects of Hypo-EVs on AEB defects in vivo chronic asthma mice and in vitro IL-4 and IL-13-induced bronchial epithelial cells, hoping to unravel the anti-asthma mechanism of aerosolized Hypo-EVs and provide solid evidence for their pharmaceutical development.

Materials and Methods

Cell Culture

HUCMSCs were generated from fresh umbilical cord samples, as we reported previously,[16] and cultured in stem cell culture medium (Cyagen, Guangzhou, China) at 37°C with 5% CO_2. Human bronchial epithelial cell line HBE135-E6E7 cells were purchased from Haixing Biological Technology (Suzhou, China) and cultured in HBE specific culture medium (Cat: TCH-G377, Haixing Biological Technology) at 37°C with 5% CO_2.

Isolation and Characterization of Hypo-EVs

Briefly, hUCMSCs were cultured for 24 h in serum-free culture medium under hypoxic (5% O_2) conditions (Hypo-MSCs).[14] The cell culture supernatants were collected and centrifuged at 300×g for 10 min and 2000×g for 20 min. Hypo-EVs were isolated by ultracentrifugation (Beckman Coulter Optima L-100 XP ultracentrifuge, Miami, FL) at 100,000×g for 90 min as previously described.[16] After that, the pellets were collected in phosphate-buffered saline (PBS) or culture medium. All centrifugations were performed at 4°C, and the Hypo-EV solution was stored at −80°C.

The shape and structure of Hypo-EVs were observed using transmission electron microscopy (JEM-1200EX; JEOL Ltd., Tokyo, Japan). The particle size distribution was detected by nanoparticle trafficking analysis using a ZetaView PMX 110 (Particle Metrix, Meerbusch, Germany), according to the manufacturer's protocols.

Animal Model Establishment and Hypo-EVs Treatment

Six-week-old female BALB/c mice were purchased from the Comparative Medicine Center of the Yangzhou University (Yangzhou, China). The mice were divided into control (normal mice), model+PBS treatment, and model+ Hypo-EV treatment groups in accordance with a random number table. For the animal model of ovalbumin (OVA)-induced asthma, mice were sensitized by intraperitoneal injection of 40 μg OVA (Sigma-Aldrich, St. Louis, MO) and 2 μg 10% aluminum

hydroxide (Sigma-Aldrich) in PBS on days 0, 7, and 14. Then, the sensitized mice were challenged with aerosolized OVA (5%) in an exposure chamber three times per week from day 21 to 53. Aerosolized OVA particles were produced by using a compression atomizer (403 M; YUWELL, Zhenjiang, China). For treatment, the mice inhaled PBS (0.5 mL PBS) or 40 μg Hypo-EVs (suspended in 0.5 mL PBS) on days 26, 33, 40, and 47. Atomization inhalation systems for PBS or Hypo-EV treatment were performed as described in our previous study.[15] After the four treatments, the mice were sacrificed on day 55 and samples were collected for further analysis.

Lung Histopathology and Immunohistochemistry

Lower right lung lobes from each mouse were fixed in 4% buffered paraformaldehyde, dehydrated with gradient ethanol, and embedded in paraffin. The 4 μm cross sections of the lungs were sectioned (3 sections per animal). The sections were subjected to hematoxylin and eosin (HE), periodic acid-Schiff (PAS), Masson staining, and immunohistochemical staining, as described previous description.[15] All images were obtained using a microscope (Nikon, Tokyo, Japan). Peribronchial inflammation and goblet cell hyperplasia scores were assessed from grades 0 to 4.[17,18] Briefly, inflammation was graded as follows: grade 0 (no inflammatory cells were observed); grade 1 (inflammatory cells were occasionally observed); grade 2 (bronchi were surrounded by 1–3 layer of inflammatory cells); grade 3 (bronchi or vessels were surrounded by 4–5 layer of inflammatory cells); grade 4 (most bronchi or vessels were surrounded by more than 5 layer of inflammatory cells). The goblet cell hyperplasia score (grades 0–4) was quantified according to the percentage of goblet cells in the epithelium: grade 0 (no goblet cells); grade 1 (<25%); grade 2 (25%–50%); grade 3 (51%–75%); and grade 4 (>75%). The percentage of collagen fibers was quantified using Image-Pro Plus software (Version X; Adobe, San Jose, CA), which was subsequently divided by the total area examined (as the percentage of collagen fibers).[19] Five bronchioles were counted on a slide for each mouse, and the mean inflammation score, goblet cell hyperplasia score, and percentage of collagen fibers were calculated for each mouse.

For immunohistochemistry, mouse lung tissue sections were incubated with an antibodies ZO-1 (GB111981, diluted 1:200; Servicebio, Wuhan, China), E-cadherin (20874-1-AP, diluted 1:500; Proteintech, Wuhan, China), Caveolin-1 (#3267, diluted 1:800; Cell Signaling Technology, Danvers, MA) overnight at 4°C, followed incubating by HRP-conjugated secondary antibody (GB23303, diluted 1:1000; Servicebio). The lung sections were then counterstained with 3.3′-diaminobenzidine and hematoxylin.

Albumin Quantification by Enzyme-Linked Immunosorbent Assay (ELISA)

100 μL of saline was added to 20 μg of lung tissue, ground completely, and centrifuged at 3000 rpm for 10 min to obtain a suspension. The concentration of albumin was quantified using an albumin ELISA Kit (Keborui, Shanghai, China) according to the manufacturer's instructions. The absorbance of the final reactant was measured at 450 nm using an ELISA plate reader (BioTek, BioTek Winooski, Vermont).

Cells Counts in Bronchoalveolar Lavage Fluid (BALF)

BALF was collected as previously described.[20] The collected BALF was centrifuged at 4 °C, 1500 rpm for 10 min, and the cell deposits were resuspended in PBS (1 mL). The total number of inflammatory cells was counted using Neubauer hemocytometer, eosinophils were counted using Wright and Giemsa staining (BASO, Zhuhai, China).

Localization of Hypo-EVs in vivo and in vitro

Hypo-EVs were labeled with DiR (Invitrogen, Carlsbad, CA) as our previous report.[21] For in vivo experiments, OVA-treated mice were nebulized with DiR-labeled Hypo-EVs (40 μg diluted in 0.5 mL PBS). After 24 h, the brain, heart, liver, spleen, lung, and kidney tissues were collected for ex vivo imaging using an Xtreme II (BRUKER, Bremen, Germany). To examine Hypo-EVs could be delivered to bronchial epithelial cells, frozen sections of lungs were prepared and then were incubated with EpCAM (GB11274-100, diluted 1: 500; Servicebio) overnight at 4 °C. After washing, Alexa Fluor 488-conjugated Goat Anti-Rabbit IgG (GB25303, diluted 1:200; Servicebio) secondary antibody was added.

For the in vitro experiments, HBE135-E6E7 cells were treated with DiR-labeled Hypo-EVs, after washing and fixing, nuclei were stained with DAPI (Beyotime, Nantong, China). The fluorescence images were visualized and captured using a Zeiss LSM 800 confocal laser scanning microscope (Zeiss, Germany).

Cell Counting Kit-8 (CCK-8) Assay

Cell viability was analyzed using CCK8 (KeyGEN BioTECH, Nanjing, China). HBE135-E6E7 cells (5×10^3 cells/well) were seeded in a 96-well plate with 100 μL of culture medium and cultured overnight. The medium was then replaced with 100 μL of culture medium in the absence or presence of Hypo-EVs (10, 20, 40μg/mL) or IL-4/IL-13 (10, 25 and 50 ng/mL) for 48 h. 10 μL of CCK-8 was added to each well, and the cells were incubated for 2 h. The absorbance of the cells in each well was measured at 450 nm using an ELISA plate reader (BioTek). Culture medium without cells was used as the blank control.

Airway Epithelial Barrier Model Establishment in vitro

Based on previous study for establishing airway epithelial barrier model in vitro,[22,23] 1.5×10^5 HBE135-E6E7 cells were seeded onto collagen (Cat: 354236, Corning, NY) coated Transwell inserts (diameter, 6.5 mm; pore size, 0.4 μm; Corning) and cultured in an atmosphere of 5% CO_2 at 37 °C. The airway epithelial barrier was successfully established after 5 days of culture. The culture medium was then removed and medium containing IL-4 and IL-13 (50 ng/mL) was added basolaterally to induce airway epithelial barrier defects.[8] IL-4 and IL-13 were purchased from Proteintech (Wuhan, China). For Hypo-EV treatment, cells were cultured in normal medium for 5 days, followed by 2 more days in the upper medium containing Hypo-EVs (40 μg/mL) and in the basolateral medium containing IL-4 and IL-13 (50 ng/mL).

FITC-Dextran Permeability Assay

Fluorescein isothiocyanate (FITC)-labeled 4-kDa dextran (2 mg/mL, Sigma-Aldrich) was added to the apical chamber, and FITC-dextran intensity in the basolateral chamber was detected after 60 min using a multifunctional microplate reader (Synergy H1, Biotek) at Ex/Em =492/520. The apparent permeability coefficient (Papp) was obtained using the equation: Papp (cm/s) = dQ/dt (V/AC_0), where dQ/dt is the permeability rate (mg/s), V is the volume of the upper chamber (cm^3), A is the upper chamber membrane surface area (cm^2), and C_0 is the initial FITC-dextran concentration in the upper chamber (mg/mL).[24]

Western Blotting

The proteins of Hypo-EVs, BEC cells, and mouse lung tissues were extracted, and the protein concentration was quantified using a BCA protein assay kit (Beyotime). Samples were separated on a different concentration (8%, 10%, 12%) sodium dodecyl-sulfate polyacrylamide gel electrophoresis (SDS-PAGE) and transferred to a polyvinylidene fluoride (PVDF) membrane. After blocking in 5% skimmed milk, membranes were incubated with the corresponding primary and secondary antibodies: TSG101 (ab133586, Abcam, Cambridge, MA), HSP70 (ab181606, Abcam), GAPDH (60004-1-Ig, Proteintech), E-cadherin (20874-1-AP, Proteintech), ZO-1 (GB111981, Servicebio), Caveolin-1 (#3267, CST), Cleaved Caspase-3 (#9661, CST), ERBB2 (18299-1-AP, Proteintech), ITGB4 (21738-1-AP, Proteintech), Claudin-18 (21126-1-AP, Proteintech), NRF2 (#12721, CST), Ezrin (26056-1-AP, Proteintech), Phospho-STAT6 (Tyr641) (AF3301, Affinity, Changzhou, China), STAT6 (BA1414, BOSTER, Wuhan, China), Goat Anti-Rabbit IgG (H+L) HRP (S0001, Affinity), Goat Anti-Mouse IgG (H+L) HRP (S0002, Affinity), then washed by TBST (Tris-buffered saline with 0.1% Tween 20). Finally, immunoblot signals were visualized using an ECL chemiluminescence kit (Beyotime). ChemiScope 3400 mini (CLINX ScienceInstruments, Shanghai, China) was used for imaging. GAPDH or Ponceau S staining was used as a loading control.[14] Band gray values were quantitated using Image J software, and the relative expression levels of proteins were normalized as the ratio of GAPDH.

Immunofluorescence

BEC cells were fixed in ice cold 100% methanol for 60 min and washed thrice with PBS. Fixed inserts were blocked with PBS, 5% normal goat serum (C0265, Beyotime), and 0.1% Triton X-100 (ST795, Beyotime) for 1 h at room temperature.

After blocking, cell monolayers were incubated with the following primary antibodies in antibody dilution buffer (PBS + 1% bovine serum albumin (BSA, ST023, Beyotime)) overnight at 4 °C: ZO-1 (GB111981, diluted 1:800; Servicebio), E-cadherin (20874-1-AP, diluted 1:500; Proteintech), Caveolin-1 (#3267, diluted 1:500; CST), and FLAG Tag (AF0036, diluted 1:100; Beyotime). The coverslips were then incubated with CoraLite488-conjugated Goat Anti-Rabbit IgG(H+L) (SA00013-2, diluted 1:600; Proteintech) and CoraLite594-conjugated Goat Anti-Rabbit IgG(H+L) (SA00013-4, diluted 1:600; Proteintech) in antibody dilution buffer for 1 h at room temperature. Finally, Nuclei were stained with DAPI (C1005, Beyotime) for 10 min. The coverslips were washed with PBS three times for 5 min each, before proceeding to the next step. Fluorescence images were obtained using a Zeiss LSM 800 confocal laser scanning microscope (Zeiss, Germany).

Transfection of siRNAs

Small interfering RNA (siRNAs) targeting Caveolin-1 and their control were designed and obtained from GenePharma (Shanghai, China). siRNA was mixed with GP-transfect-Mate (GenePharma) in OptiMEM (Gibco) to form complexes and then transfected into the Hypo-MSCs as previous description.[25] CAV-1 expression in Hypo-MSCs was examined with WB. The culture medium was collected, and Hypo-EV CAV1-knockdown (EVs-KD) were isolated and purified as described above.

Lentiviral Overexpression

The lentiviral vector, Ubi-MCS-3FLAG-CBh-gcGFP-IRES-puromycin (GV492), was designed and constructed using GeneChem (Shanghai, China). For Caveolin-1 overexpression cell line, Caveolin-1 lentiviruses were transfected into hUCMSCs or BEC according to the manufacturer's instructions.

Real-Time Fluorescent Quantitative PCR

Total RNA was extracted using RNAiso Plus (Takara Dalian Bio). HiScript II Q RT SuperMix (Vazyme, Nanjing, China) was used to synthesize complementary DNA (cDNA) via reverse transcription. Real-time PCR was performed using the ChamQ Universal SYBR qPCR Master Mix (Vazyme). All primers for real-time PCR, including GAPDH, IL-4, IL-5, IL-13 and CAV-1 were designed and purchased from Tsingke Biotech Co., Ltd. (Nanjing, China). Each gene was normalized to GAPDH mRNA levels and the data were calculated using the $2^{-\Delta\Delta Ct}$ method.[26]

Statistical Analysis

Data were analyzed using the GraphPad Prism software (version 5; La Jolla, Calif). Data are presented as the mean ± SD. The groups were compared using the Student's *t* test, and One-way analysis of variance (Tukey Kramer post hoc test) was used for studies with more than two groups. Statistical significance was set at $P < 0.05$.

Results

Nebulization of Hypo-EVs Alleviated Airway Inflammation and Remodeling, as well as Epithelial Barrier Defects in Chronic Asthma Mice

The isolated Hypo-EVs were identified using transmission electron microscopy (TEM), nanoparticle tracking analysis, and Western blotting. Hypo-EVs showed a typical cup-shaped morphology with a diameter of approximately 134 nm (Figure 1A) and expressed EV markers, such as heat-shock protein 70 (HSP70) and tumor susceptibility gene 101 (TSG101) (Figure 1B). First, we explored the effect of atomized Hypo-EVs on airway pathology in asthmatic mice (Figure 1C), and consistent with our previous report,[15] compared with PBS treatment (OVA+PBS group), the mice treated with Hypo-EVs (OVA+Hypo-EVs group) displayed reduced peribronchial cellular infiltration, mucus hypersecretion, and collagen deposition as determined by HE, PAS, and Masson staining for lung tissues, respectively (Figure 1D and E). Additionally, the numbers of total inflammatory cells and eosinophils in bronchoalveolar lavage fluid (BALF) were significantly decreased by Hypo-EV administration (Supplementary Figure S1), suggesting that nebulization of Hypo-EVs could alleviate airway inflammation and remodeling.

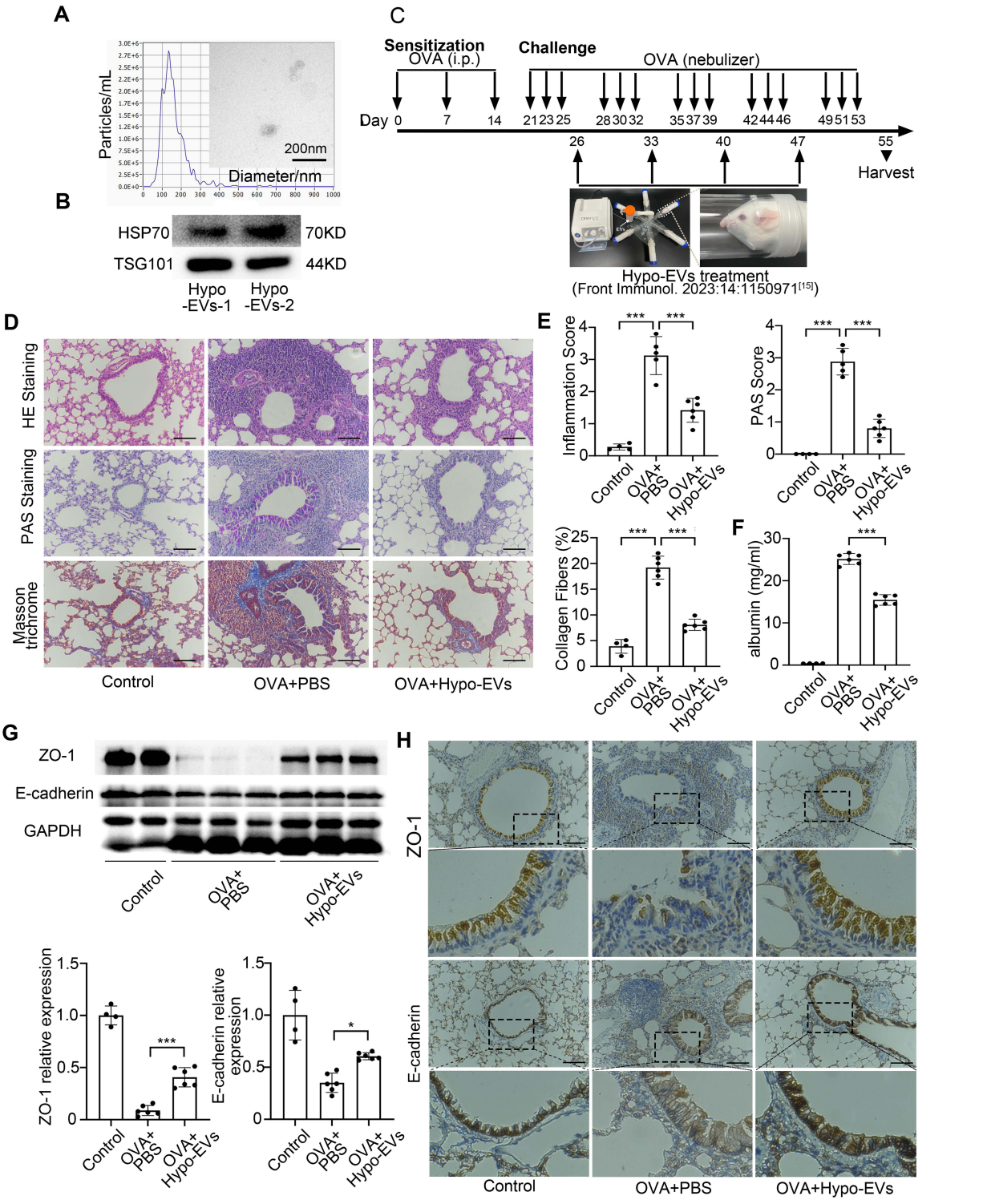

Figure 1 Effect of atomized Hypo-EVs on the airway barrier defects in OVA-induced asthma mice. (**A**) Transmission electron microscopy (TEM) image of morphology and nanoparticle tracking analyses (NTA) of size distributions for Hypo-EVs. Scale bar: 200 nm. (**B**) EVs markers (HSP70, TSG101) were detected by Western blot. (**C**) Experimental protocol for the development of chronic allergic asthma and treatment with Hypo-EVs. (**D**) Representative photographs of HE, PAS and Masson trichrome stained lung sections from each group (black bars: 100 μm), the images are shown at × 200. (**E**) The inflammatory infiltration was quantified by inflammation score, the goblet cell hyperplasia was quantified by PAS score, and the percentage of collagen fiber content in airway was measured (n = 4–6 per group). (**F**) Airway leakiness was assessed via quantification of albumin in the fluid from mouse lung grinding by ELISA (n = 4–6 per group). (**G**) OVA mice exposed to aerosolized Hyo-EVs exhibit an increment in ZO-1 and E-cadherin protein in the lung as measured by Western blot (n = 4–6 per group). (**H**) Representative × 200 (up) and × 400 (down) images of mouse airways immunostained for ZO-1 and E-cadherin. Scale bars: 100 μm. *$P < 0.05$; ***$P < 0.001$.

Abbreviations: Hypo-EVs, hypoxic hUCMSC-derived EVs; MSCs, mesenchymal stem cells; hUCMSCs, human umbilical cord MSCs; EVs, extracellular vesicles; HSP70, heat shock protein 70; TSG101, tumor susceptibility gene 101; i.p., intraperitoneal injection; PBS, phosphate-buffered saline; OVA, ovalbumin; HE, hematoxylin and eosin; Masson, Masson trichrome staining; PAS, Periodic Acid-Schiff.

Next, the airway epithelial barrier protective efficacy of Hypo-EVs in mice with chronic asthma was investigated. We measured albumin concentration in the lung, which is an indicator of protein permeability across the airway epithelium, and found that Hypo-EV administration dramatically decreased albumin levels compared to PBS treatment (Figure 1F). To determine whether junction formation is regulated by Hypo-EVs, ZO-1 (a tight junction marker) and E-cadherin (an adherens junction marker) were detected in mouse lungs. WB analysis showed that Hypo-EV treatment significantly increased ZO-1 and E-cadherin expression (Figure 1G). Histochemical results showed a similar trend, but further showed that ZO-1 and E-cadherin were predominantly localized in bronchial epithelial cells (Figure 1H). These data suggest that the nebulization of Hypo-EVs ameliorates epithelial barrier defects in mice with chronic asthma.

Hypo-EVs Could Be Taken Up by Bronchial Epithelial Cells (BEC)

To investigate whether the protective effect of Hypo-EVs on the airway epithelial barrier was associated with the direct regulation of BEC, the uptake of Hypo-EVs by BECs in vivo was evaluated. DiR-labeled Hypo-EVs were administered via the nebulized route in a mouse model of OVA-induced lung injury (Figure 2A). After 24 h, the fluorescence intensity was observed in the excised lungs, with no intensity in the brain, heart, liver, kidney, or spleen (Figure 2B). Frozen sections of the mouse lungs were prepared, and the airway epithelial cell-specific marker EpCAM was used to stain the epithelial cells. The results revealed that the DiR-labeled Hypo-EVs (red) colocalized with bronchial epithelial cells (green) (Figure 2C), indicating that aerosolized Hypo-EVs could be delivered to the lungs and taken up by BEC.

Base on the methodology outlined by Bandeira et al[27] the BALF was collected from mice and subsequently subjected to ultracentrifugation to remove the EVs. Then, Hypo-EVs were incubated in EVs-free BALF for 7 days at 37°C, after which TEM analysis was performed. As shown in Supplementary Figure S2, the structure of EVs is integrity, confirming the stability of Hypo-EVs in the lung environment and indicating, at least in part, that the internal contents of Hypo-EVs remain intact prior to entering the airway epithelial cell.

To verify Hypo-EVs can be taken up by BEC in vitro, HBE135-E6E7 cells, a human BEC line commonly used as a model for respiratory epithelial diseases,[28] were selected and co-cultured with DiR-labeled Hypo-EVs, and as expected, DiR-labeled EVs were internalized by BEC (Figure 2D).

Hypo-EV Treatment Attenuated IL-4 and IL-13 (IL-4/IL-13)-Induced Airway Epithelial Permeability and Enhanced ZO-1 and E-Cadherin Expression in vitro

The effects of Hypo-EVs on airway epithelial barrier defects were tested in vitro. IL-4 and IL-13, classical type-2 cytokines that play vital roles in the pathogenesis of asthma, are utilized as BEC stimulators to establish airway epithelial barrier defects.[8] First, the cytotoxicity of Hypo-EVs and IL-4/IL-13 toward BEC was investigated using the CCK8 assay and by detecting cleaved Caspase-3. As shown in Figure 3A and B, compared to the control treatment (0 group), none of the concentrations of Hypo-EVs (10, 20, and 40 ug/mL) had an impact on cell viability and cleaved Caspase-3 expression, and IL-4/IL-13 (both 50 ng/mL) did not have a cytotoxic effect. Next, HBE135-E6E7 cells were cultured in a transwell liquid-liquid interface culture system to establish a bronchial epithelial cell monolayer.[22,23] Changes in epithelial barrier function were assessed by measuring the permeability of 4 kDa FITC-Dextran, and as shown in Figure 3C, the epithelial cell permeability gradually increased after IL-4/IL-13 stimulation as seen by more 4kDa FITC-dextran leak. Interestingly, Hypo-EV treatment significantly inhibited the increase in epithelial cell permeability in a dose dependent manner (Figure 3D and Supplementary Figure S3), consequently, the subsequent experiments were conducted with a Hypo-EV concentration of 40 μg/mL. Furthermore, the 40 μg/mL Hypo-EV concentration was observed to have no impact on the regulation of IL-4 and IL-13 expression in HBE135-E6E7 cells (Supplementary Figure S4).

Next, we assessed the expression of junctional proteins ZO-1 and E-cadherin in each group. WB results showed that IL-4/IL-13 stimulation led to the downregulation of ZO-1 and E-cadherin, while these two proteins were dramatically restored by Hypo-EV treatment (Figure 3E). Immunofluorescence staining results showed that ZO-1 and E-cadherin were localized in the membranes of neighboring epithelial cells, showing continuous distribution in the control group, while the fluorescence intensity decreased and distribution was discontinuous in the membranes of IL-4/IL-13-treated BEC. Compared with the IL-4/IL-13-treated group, the fluorescence intensity of these two proteins was higher, and their

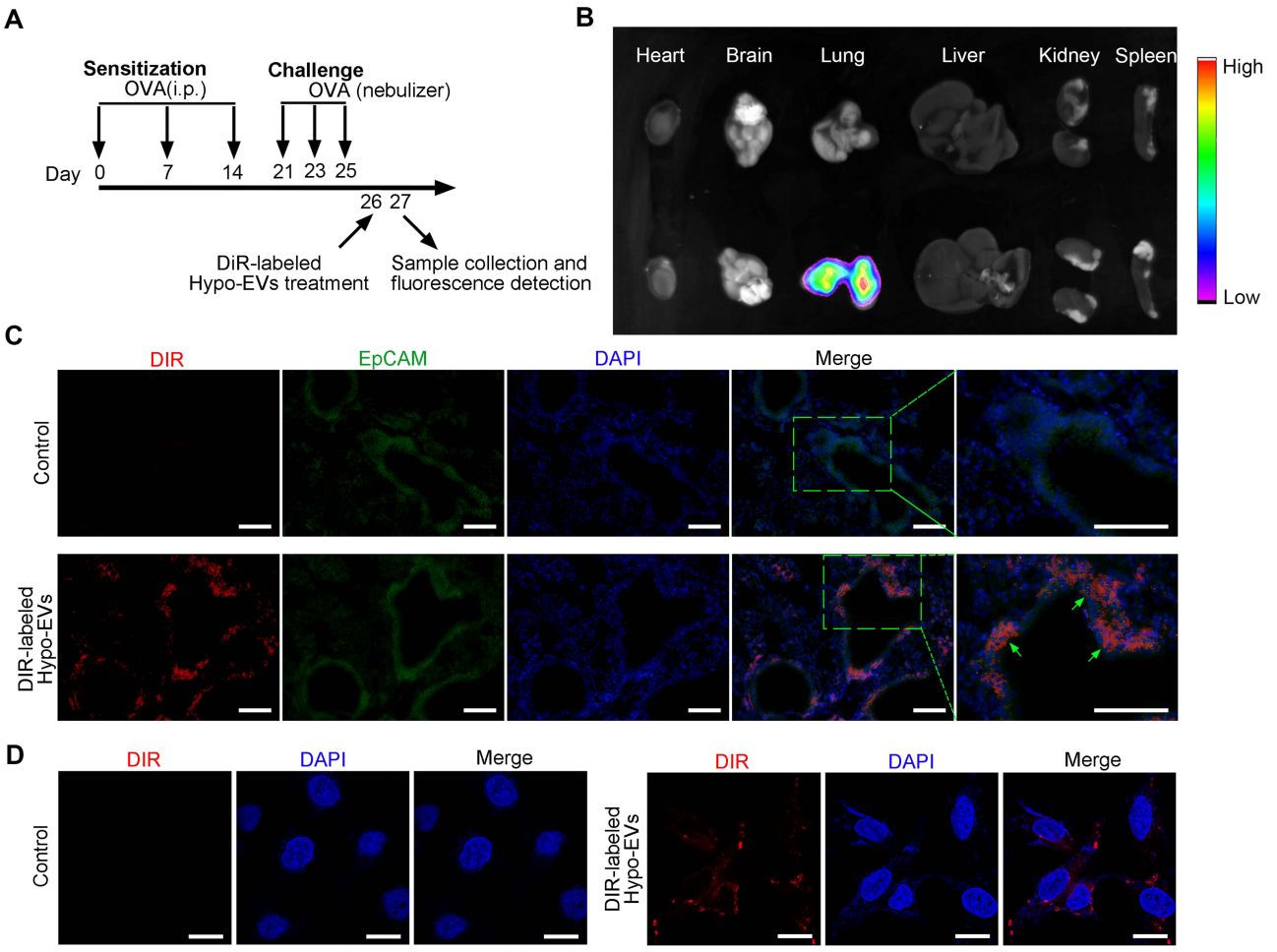

Figure 2 Hypo-EVs could be taken up by bronchial epithelial cells in vivo and in vitro. (**A**) The timeline of OVA exposure and DiR-labeled Hypo-EVs treatment. (**B**) Biodistribution of DiR-labeled Hypo-EVs in heart, brain, lung, liver, kidney and spleen was visualized at 1 day after nebulized inhalation administration. (**C**) EpCAM (green, a marker of epithelial cell) were detected to track the uptake of DiR-labeled Hypo-EVs (red) in lung sections (arrow pointing) by immunofluorescence staining. Scale bar: 50 μm. (**D**) The internalization of DiR-labeled Hypo-EVs into BEC cells is observed with a confocal microscope. Scale bar: 20 μm.

Abbreviations: OVA, ovalbumin; i.p., intraperitoneal injection; Hypo-EVs, hypoxic hUCMSC-derived EVs; MSCs, mesenchymal stem cells; hUCMSCs, human umbilical cord MSCs; EVs, extracellular vesicles; EpCAM, epithelial cell adhesion molecule; DAPI, 4′,6-diamidino-2-phenylindole.

distribution was continuous in the Hypo-EV treatment group (Figure 3F). Altogether, these findings suggest that Hypo-EVs have a direct protective effect on the airway epithelial barrier, which may be related to the upregulation of junctional proteins.

Hypo-EVs Alleviated Airway Epithelial Barrier Defects by Transferring CAV-1

EVs play a vital role in cellular communication by transferring their contents, such as proteins,[29,30] and recent years, accumulating evidence has confirmed that some proteins, such as erythroblastosis oncogene B2 (ERBB2),[31] integrin β4 (ITGB4),[32] Caveolin-1 (CAV-1),[33] Claudin-18,[34] Nuclear erythroid 2-related factor 2 (NRF2)[35] and Ezrin[36] emerged protective functions on the epithelial barrier in asthma. We applied the WB method to detect the expression of the six proteins mentioned above as well as ZO-1 and E-cadherin in Hypo-EVs. As shown in Figure 4A, in the case of consistent sample amounts of Hypo-EVs (TSG101 gray scale is equal), a strong band intensity of CAV-1 was observed, the abundance of Ezrin was lower, and the other proteins were not expressed. Therefore, we speculated that Hypo-EVs might promote airway epithelial barrier integrity by delivering CAV-1. Indeed, the protein levels of CAV-1 were significantly increased in IL-4/IL-13-treated BEC after treatment with Hypo-EVs (Figure 4B). Additionally, the immunofluorescence staining signals of CAV-1 in IL-4/IL-13-treated BEC were decreased, but recovered by Hypo-EV treatment (Figure 4C). More importantly, anti-flag staining of BEC treated with Hypo-EVs containing CAV-1^{-flag} showed that red fluorescence

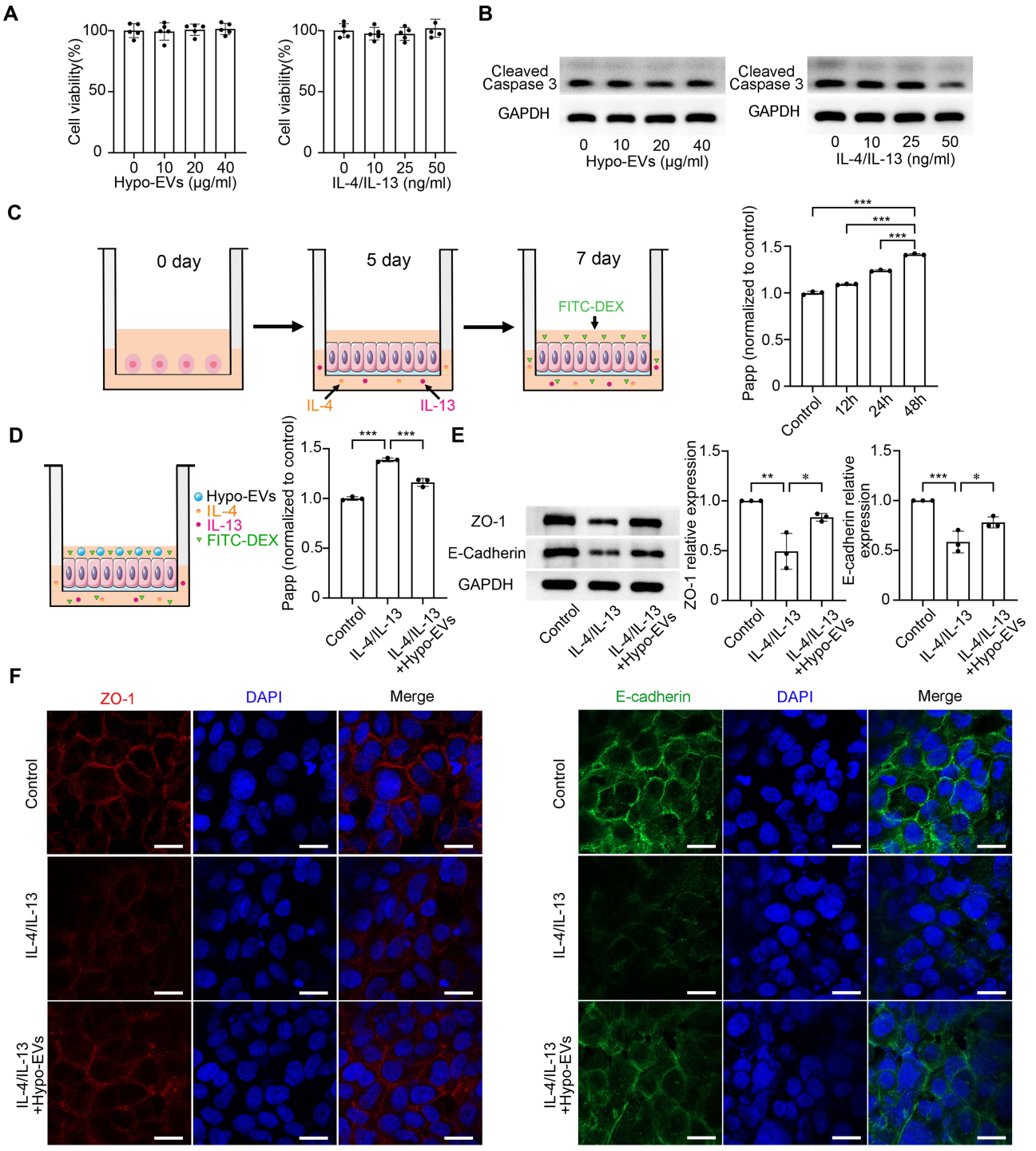

Figure 3 Hypo-EV administration decreased leakage of IL-4/IL-13-induced BEC monolayer and increased ZO-1 and E-cadherin protein expression. (**A**) HBE135-E6E7 cells were treated with Hypo-EVs or IL-4/IL-13 for 48 h. The cell viability was analyzed by CCK-8 assay (n = 4–5 per group). (**B**) HBE135-E6E7 cells were treated with Hypo-EVs or IL-4/IL-13 for 48 h. The protein levels of Cleaved caspase 3 were analyzed by Western blotting. (**C**) Sketch of transwell assay and the relative IL-4/IL-13-induced BEC monolayer leakage. Apparent permeability coefficient (Papp) of FITC-DEX were measured (n = 3 per group). (**D**) HBE135-E6E7 cell monolayers were treated with IL-4/IL-13 and Hypo-EVs for 48 h, then the Papp of FITC-DEX were detected (n = 3 per group). (**E**) ZO-1 and E-cadherin protein expression were determined by Western blot. Data was derived from the results of three independent repeated experiments. (**F**) HBE135-E6E7 cell monolayers were fixed and subjected to immunofluorescence analysis to detect ZO-1 and E-cadherin. The nuclei were stained with DAPI. Images were obtained using a confocal microscope. Scale bar: 20 μm. *$P < 0.05$, **$P < 0.01$, ***$P < 0.001$. **Abbreviations**: Hypo-EVs, hypoxic hUCMSC-derived EVs; MSCs, mesenchymal stem cells; hUCMSCs, human umbilical cord MSCs; EVs, extracellular vesicles; IL, interleukin; Papp, apparent permeability coefficient; FITC, Fluorescein isothiocyanate; DEX, dextran; DAPI, 4′,6-diamidino-2-phenylindole.

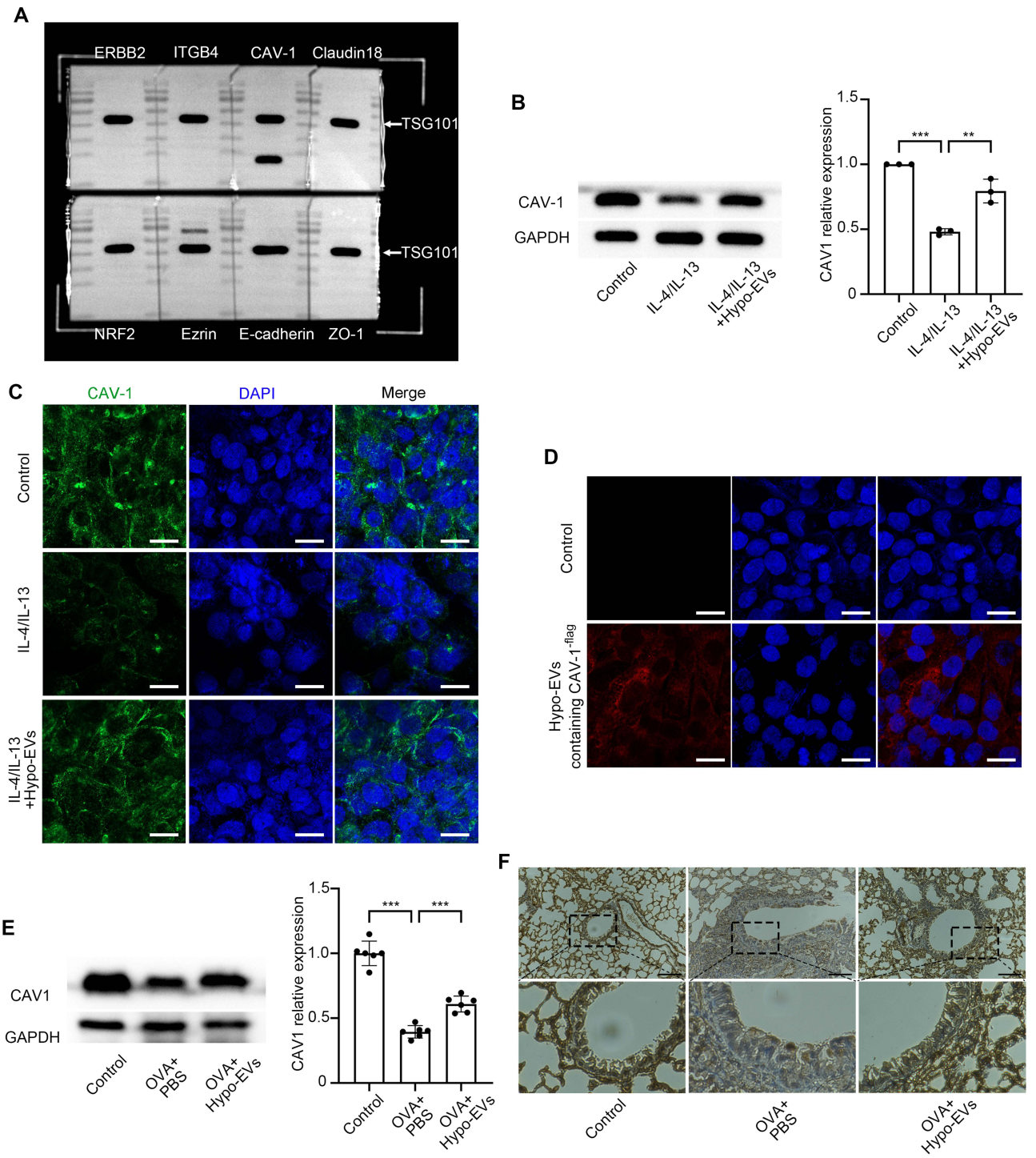

Figure 4 CAV-1 in Hypo-EVs could be transferred into epithelial cells. (**A**) Western blot analysis of ERBB2, ITGB4, CAV1, Claudin-18, NRF2, Ezrin, E-cadherin, and ZO-1 in Hypo-EVs. TSG101 was used as a loading control. (**B**) CAV-1 protein levels in BEC with or without Hypo-EVs after co-culturing for 48 h. Data was derived from the results of three independent repeated experiments. (**C**) CAV-1 protein expression and distribution in each group were determined using immunofluorescence staining. Scale bar: 20 μm. (**D**) EVs from Hypo-MSCs that had been transfected with CAV-1-^{flag} lentiviral vector was added to BEC cells for 6 h, then immunofluorescence staining was performed using anti-flag antibody. Scale bars: 20 μm. (**E**) CAV-1 protein expression in each mice group were detected (n = 6 per group). (**F**) CAV-1 expression in every group was determined by using immunohistochemistry staining. Scale bar: 100 μm. $^{**}P < 0.01$, $^{***}P < 0.001$.

Abbreviations: ERBB2, erythroblastosis oncogene B2; ITGB4, integrin β4; CAV-1, caveolin-1; NRF2, nuclear erythroid 2-related factor 2; IL, interleukin; Hypo-EVs, hypoxic hUCMSC-derived EVs; MSCs, mesenchymal stem cells; hUCMSCs, human umbilical cord MSCs; EVs, extracellular vesicles; GAPDH, glyceraldehyde-3-phosphate dehydrogenase; PBS, phosphate-buffered saline; OVA, ovalbumin.

was located in the cytoplasm of BEC (Figure 4D), suggesting that CAV-1 can be transferred into BEC through Hypo-EVs. We also detected the CAV-1 expression in mice. Western blotting results showed that CAV-1 expression in the lungs of OVA mice was significantly enhanced by Hypo-EV administration (Figure 4E). Histochemical results revealed that CAV-1 presented a weak signal in PBS-treated mouse lungs, which was partially salvaged by Hypo-EV treatment (Figure 4F).

To circumvent the issue of off-target effects, four distinct siRNAs targeting CAV-1 (siRNA308, siRNA439, siRNA788, and siRNA1074) were constructed and transfected into hypoxic hUCMSCs to knockdown CAV-1 expression. Their knockdown efficacy was validated through real-time PCR and Western blot, and the results showed that siRNA308 was the most effective (Figure 5A and Supplementary Figure S5). Thus, we selected siRNA308 to transfect MSC to produce Hypo-EVs with CAV-1 knockdown (EVs-KD), and as shown in Figure 5B, compared with Hypo-EVs with siRNA control (EVs-NC), the protein level of CAV-1 in EVs-KD was decreased. To further elucidate the role of Hypo-EV-derived CAV-1 in barrier protection in asthma, we compared the role of EVs-NC and EVs-KD in the regulation of barrier permeability and the expression of junctional proteins in vitro and in vivo. The decrease in FITC-dextran leakage in the EVs-NC treatment group was reversed by CAV-1 knockdown (Figure 5C). ZO-1 and E-cadherin upregulation by EVs-NC treatment was also reversed by CAV-1 knockdown (Figure 5D and E). Furthermore, the EVs-NC-mediated decrease in albumin levels was altered by CAV-1 knockdown in the lungs of asthmatic mice (Figure 5F). Compared with the EVs-NC group, the protein levels of ZO-1 and E-cadherin in the mouse lungs were reduced (Figure 5G and H). Taken together, these results suggest that CAV-1 plays a crucial role in Hypo-EV-mediated protection of the airway epithelial barrier.

CAV-1 Knockdown Impaired the Improvement Effect of Hypo-EVs on Airway Inflammation and Airway Remodeling in Chronic Asthma Mice

To identify whether CAV-1 was responsible for the beneficial effects of Hypo-EVs on airway inflammation and remodeling, EVs-KD or their control EVs-NC were nebulized in OVA-induced asthmatic mice (Figure 6A). Our results showed that the degree of increase in inflammation, PAS score, area of collagen fibers (Figure 6B and C), number of total cells and eosinophils (Figure 6D), and expression of IL-4, IL-5, and IL-13 (Figure 6E) in EVs-KD-treated mice was higher than that in EVs-NC-treated mice. These findings demonstrated that decreased CAV-1 expression impairs Hypo-EV-mediated lung protection.

Hypo-EV-Derived CAV-1 Inhibited the Expression of Phosphorylation STAT6 (p-STAT6)

STAT3 and STAT6 have been reported to be downstream of IL-4 and IL-13 signaling,[37] thus BEC monolayers were pretreated with a STAT3 inhibitor (Stattic) or STAT6 inhibitor (AS1517499) to determine the underlying mechanisms responsible for cytokine-induced epithelial injury. As shown in Figure 7A, cytokine-induced downregulation of ZO-1 and E-cadherin proteins was abolished by a STAT6 inhibitor rather than by a STAT3 inhibitor, suggesting that STAT6 might be the key mediator of cytokine-mediated epithelial barrier defects. Indeed, the STAT6 inhibitor inhibited airway epithelial permeability induced by type-2 cytokines (Figure 7B).

CAV-1 has the function of regulating signals,[38] therefore, we investigated whether STAT6 signaling could be influenced by CAV-1. The protein levels of CAV-1 in BEC were upregulated following transfection with lentiviral particles for CAV-1 overexpression (LV-CAV-1) (Figure 7C). WB results showed that CAV-1 overexpression significantly reduced the levels of p-STAT6 in IL-4/IL-13-treated BEC (Figure 7D), whereas the expression of ZO-1 and E-cadherin was increased (Figure 7E). Since CAV-1 can play a role in cell survival in specialized cells, thus the viability and the Cleaved Caspase 3 expression were also detected in LV-CAV-1-BEC cells. As shown in Supplementary Figures S6 and S7, overexpression of CAV-1 did not result in any discernible impact on BEC cell activity or Cleaved caspase 3 expression, regardless of the absence or presence of IL-4/IL-13 stimulation, suggesting that the regulation of epithelial barrier proteins (ZO-1 and E-cadherin) by CAV-1 in BEC cells is not linked to its control of cell survival and programmed cell death. Additionally, we found that p-STAT6 levels were inhibited by Hypo-EV treatment in vitro in IL-4/IL-13-induced BEC and in vivo in

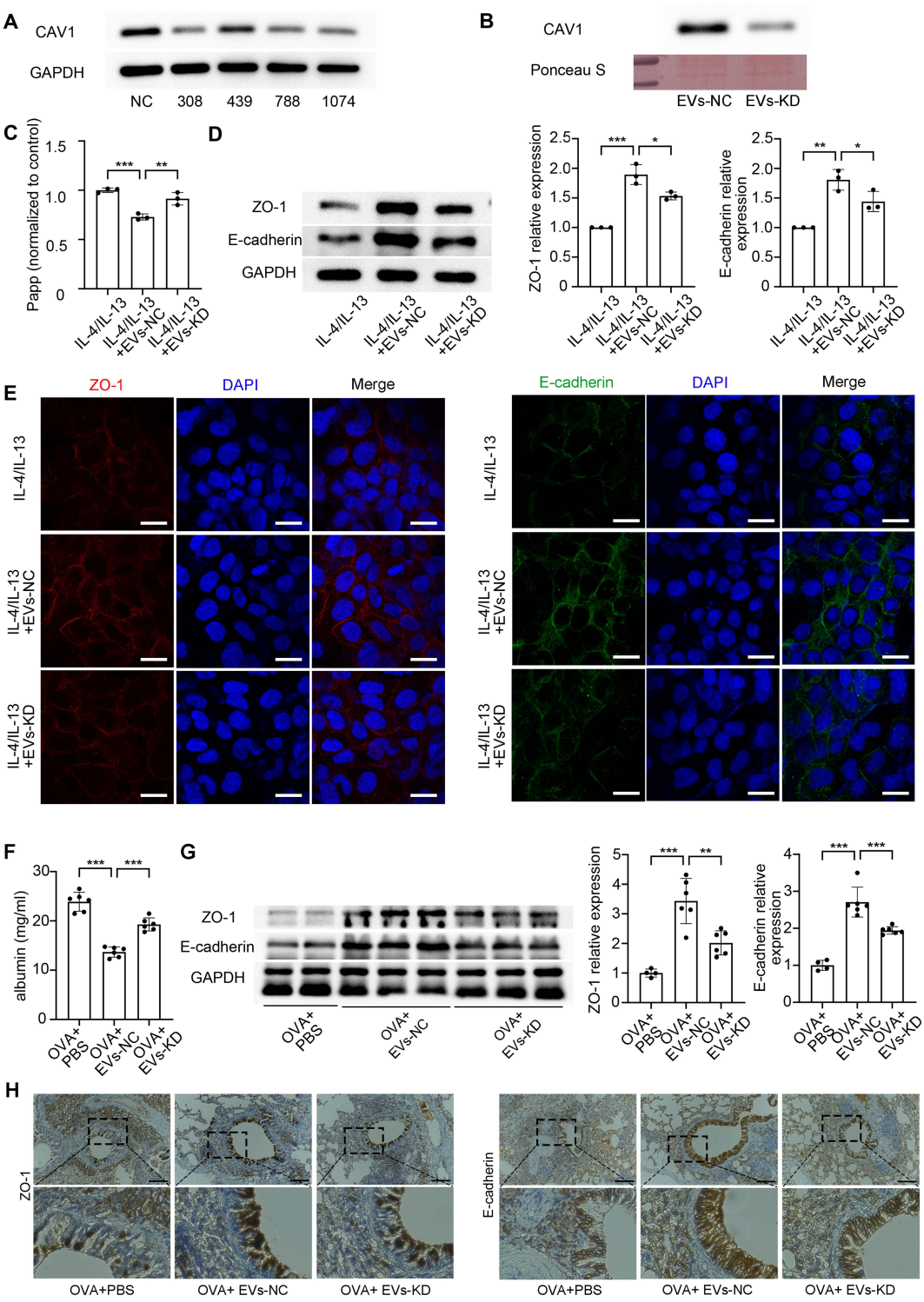

Figure 5 Knockdown of CAV-1 impaired Hypo-EVs-mediated protect effect on airway epithelial barrier in vitro and in vivo. (**A**) Western blot analysis of CAV1 expression in Hypo-MSCs transfected with control siRNA (NC) or CAV-1 siRNAs (308, 439, 788, 1074). (**B**) Western blot analysis of CAV1 expression in Hypo-EVs with CAV-1 knockdown (EVs-KD) and their control Hypo-EVs with siRNA control (EVs-NC). Ponceau S staining served as a loading control. (**C**) BEC monolayers were treated with IL-4/IL-13 and EVs-NC or EVs-KD for 48h, then the Papp of FITC-DEX were detected (n = 3 per group). (**D**) The ZO-1 and E-cadherin protein expression in each group were determined using Western blot. Data was derived from the results of three independent repeated experiments. (**E**) The protein expression of ZO-1 and E-cadherin were detected using immunofluorescence staining. Scale bar: 20 μm. (**F**) The concentrations of albumin in mice were quantified by using ELISA (n = 6 per group). (**G**) ZO-1 and E-cadherin expression from lung tissues of mice in OVA, OVA+EVs-NC, and OVA+EVs-KD group were detected by using Western blot (n = 4–6 per group). (**H**) Immunohistochemistry staining was performed to detect the expression of ZO-1 and E-cadherin in lung tissues of mice. Scale bar: 100 μm. **P* < 0.05, ***P* < 0.01, ****P* < 0.001.

Abbreviations: CAV-1, caveolin-1; IL, interleukin; GAPDH, glyceraldehyde-3-phosphate dehydrogenase; PBS, phosphate-buffered saline; OVA, ovalbumin; EVs-KD, Hypo-EVs with CAV-1 knockdown; EVs-NC, Hypo-EVs with siRNA control; DAPI, 4′,6-diamidino-2-phenylindole.

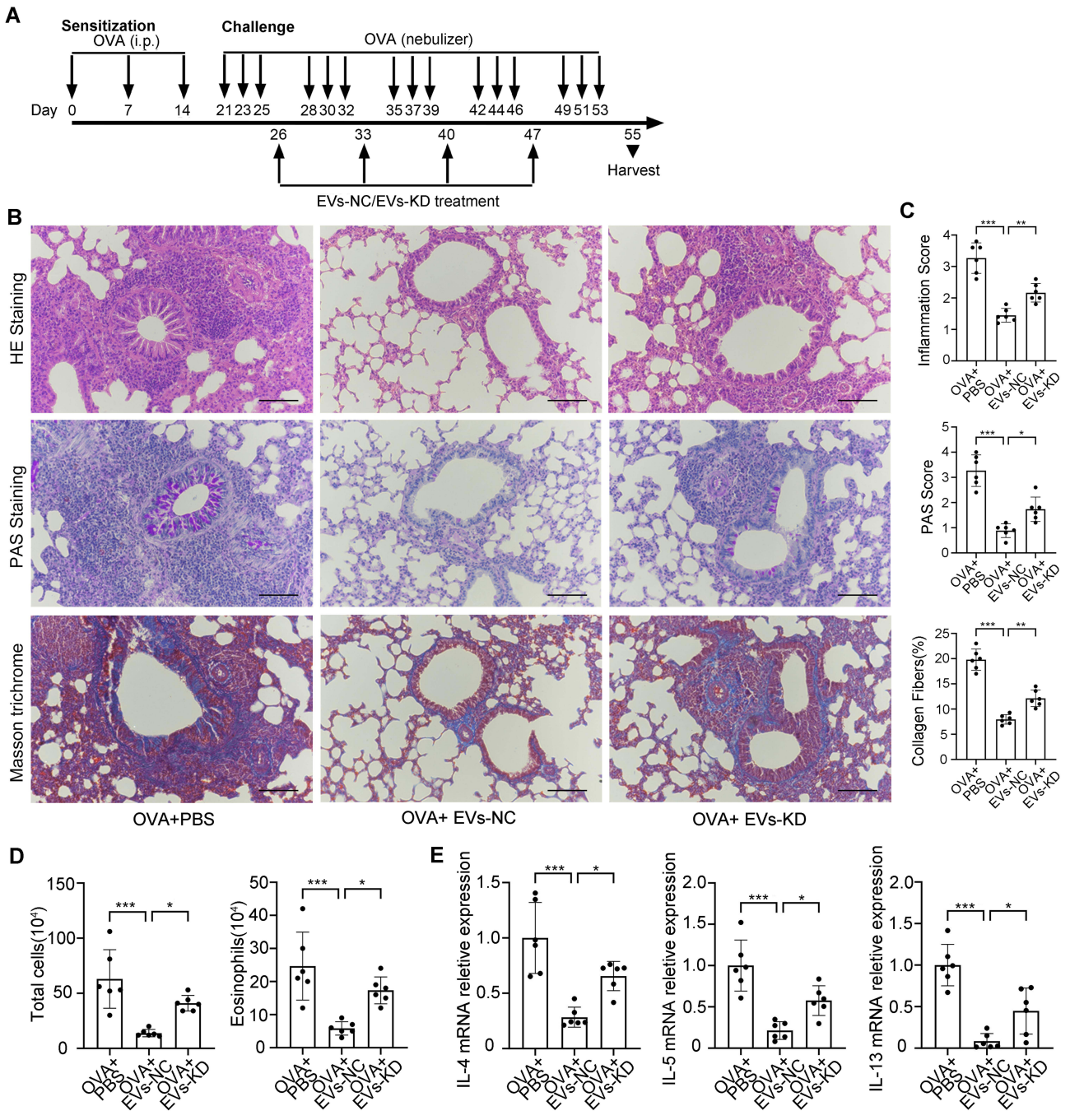

Figure 6 CAV-1 knockdown impaired the improvement effect of Hypo-EVs on airway inflammation and airway remodeling in chronic asthma mice. (**A**) Schematic diagram of animal experimental procedure in OVA mice. (**B**) Representative HE staining, PAS staining, Masson trichrome of lung sections from each group, scale bar: 100 μm. (**C**) The corresponding inflammation score, PAS score, and the percentage of collagen fiber content from each group were analyzed (n = 6 per group). (**D**) Total cells and eosinophils numbers in each group were counted (n = 6 per group). (**E**) Levels of IL-4, IL-5 and IL-13 mRNA in lung tissues of mice were measured by real-time PCR (n = 6 per group). $^{*}P < 0.05$, $^{**}P < 0.01$, $^{***}P < 0.001$.

Abbreviations: IL, interleukin; OVA, ovalbumin; EVs-KD, Hypo-EVs with CAV-1 knockdown; EVs-NC, Hypo-EVs with siRNA control; Hypo-EVs, hypoxic hUCMSC-derived EVs; i.p., intraperitoneal injection; HE, hematoxylin and eosin; Masson, Masson trichrome staining; PAS, Periodic Acid-Schiff.

asthmatic mouse lungs (Figure 7F and G). Furthermore, EVs-KD significantly increased the protein expression of p-STAT6 compared to that in the EVs-NC group (Figure 7H and I). Taken together, these results indicated that Hypo-EVs prevented type-2-cytokine-induced barrier defects in BEC via CAV-1-mediated p-STAT6 inhibition.

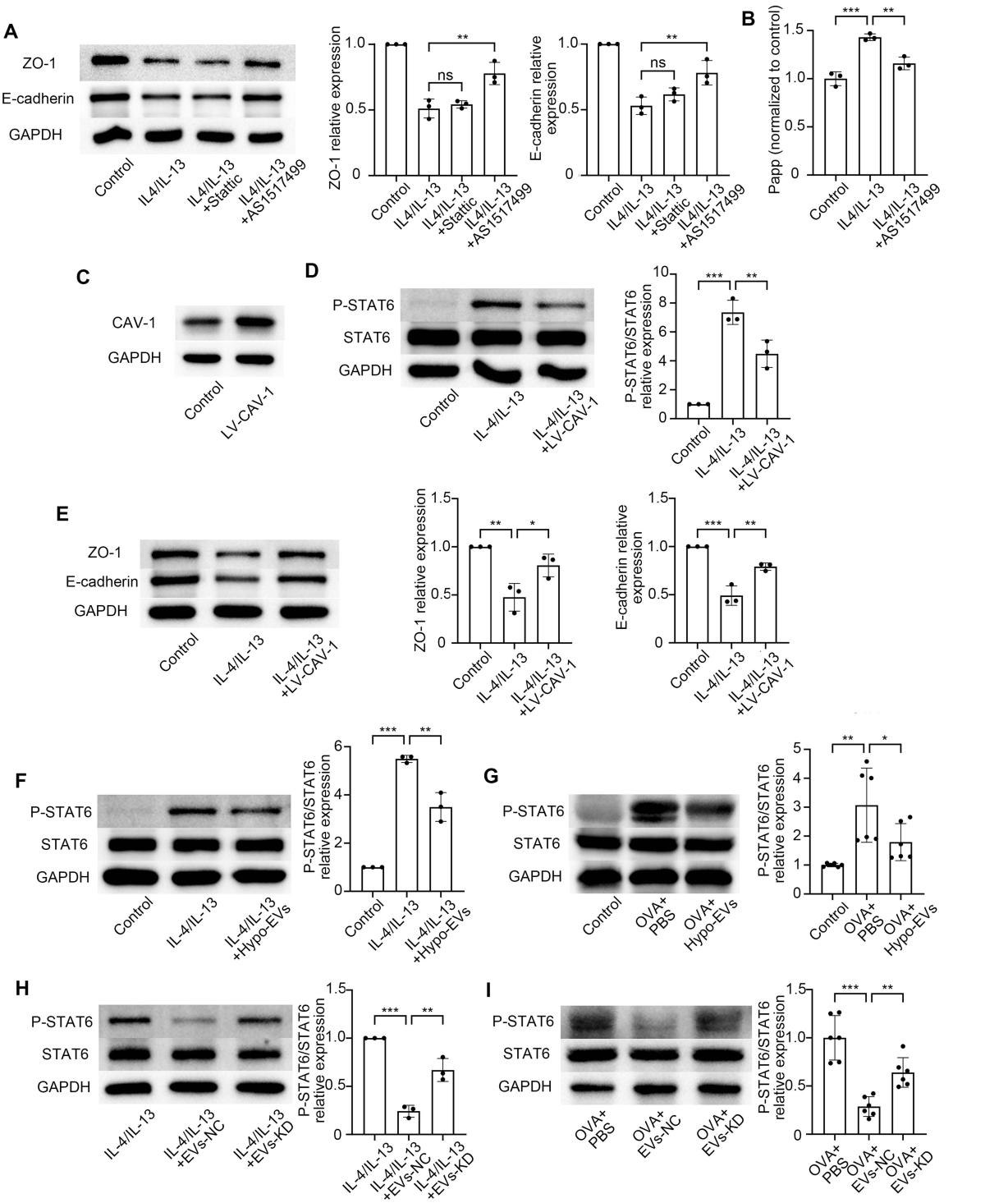

Figure 7 CAV-1 inhibited the expression of p-STAT6. HBE135-E6E7 monolayers were pretreated with STAT6 inhibitor (100 nM of AS1517499) or STAT3 inhibitor (10 μM of Stattic) for 30 min before the cytokine treatment for 48 h. (**A**) Western blot analysis of ZO-1 and E-cadherin expression in each group. Data was derived from the results of three independent repeated experiments. (**B**) Papp of HBE135-E6E7 monolayers were detected after treated with IL-4/IL-13 in the presence or absence of AS1517499 (n = 3 per group). (**C**) Western blot showing the CAV-1 levels in lentiviral infected HBE135-E6E7 cells. (**D**) Western blot analysis showing the levels of p-STAT6 and STAT6 in each cell groups. Data was derived from the results of three independent repeated experiments. (**E**) Western blot analysis showing the levels of ZO-1 and E-cadherin in each cell groups. Data was derived from the results of three independent repeated experiments. (**F**) Western blot analysis of protein level of p-STAT6 and STAT6 in control, IL-4/IL-13-treated group, and IL-4/IL-13+Hypo-EVs group. Data was derived from the results of three independent repeated experiments. (**G**) Western blot of p-STAT6 and STAT6 in mice lung tissues (n = 4–6 per group). (**H**) WB analysis of protein level of p-STAT6 and STAT6 in IL-4/IL-13-treated cells, IL-4/IL-13+EVs-NC, and IL-4/IL-13+EVs-KD. Data was derived from the results of three independent repeated experiments. (**I**) Western blot of p-STAT6 and STAT6 from lung tissues of mice in PBS, EVs-NC, and EVs-KD group (n = 6 per group). **P* < 0.05, ***P* < 0.01, ****P* < 0.001.
Abbreviations: CAV-1, caveolin-1; IL, interleukin; GAPDH, glyceraldehyde-3-phosphate dehydrogenase; PBS, phosphate-buffered saline; OVA, ovalbumin; EVs-KD, Hypo-EVs with CAV-1 knockdown; EVs-NC, Hypo-EVs with siRNA control; Hypo-EVs, hypoxic hUCMSC-derived EVs; STAT6, signal transducer and activator of transcription 6; p-STAT6, Phospho-Stat6; LV, lentiviral.

Discussion

Airway epithelial barrier defects contribute to asthma initiation, persistence and exacerbation,[5,6] therefore they have been emphasized as attractive therapeutic targets.[10] As a novel nanomedicine, MSC-EVs exerted lung-protective effects in asthmatic mice,[13] however, whether MSC-EVs can alleviate airway epithelial barrier defects in asthma remained unknown. We previously reported that nebulization of hypoxic hUCMSC-EVs (Hypo-EVs) could effectively attenuate airway inflammation and remodeling in chronic asthma mice, providing a promising noninvasive MSC-EV-based treatment approach for asthma disease.[15] In this study, we further investigated the therapeutic efficacy of Hypo-EVs in airway epithelial barriers. Our results showed that in vivo aerosolized Hypo-EVs could be delivered to airway epithelial cells and significantly decreased the levels of albumin in mouse lungs, concomitant with an increased expression of E-cadherin and ZO-1 proteins. In vitro, Hypo-EVs dramatically suppressed the reduction of E-cadherin and ZO-1, and the increases in FD4 permeability in HBE135-E6E7 cells induced by IL-4/IL-13. These data strongly indicate that Hypo-EVs can directly and effectively protect airway epithelial barrier function under asthmatic conditions. Additionally, apart from increasing epithelial permeability,[8] type-2 cytokines also induce eosinophil recruitment, goblet cell hyperplasia, and extracellular matrix deposition.[39] Together with previous findings that atomized Hypo-EVs notably reduced the levels of IL-4, IL-5, and IL-13 in alveolar lavage fluid,[15] we supposed that atomized Hypo-EVs could directly act on airway epithelial cells and promote epithelial barrier repair, thereby reducing the deposition of allergen (OVA) and the subsequent increase in the levels of type-2 cytokines, eventually improving airway pathology, which might be the lung-protective process of Hypo-EVs in OVA-asthma mice.

A more recent study reported that the inhalation administration of EVs permits their distribution to the distal lungs, where they are transported to the circulatory system via the alveolar-capillary barrier.[40] Additionally, EVs have the potential to prompt target cells to release functional EVs.[41] Thus, it can be postulated that atomized Hypo-EVs may also gain access to the bloodstream, potentially leading to the release of EVs from other cells and thus intensifying their impact on the airways of a chronic asthma mouse model, which requires further experimental confirmation.

It has been reported that MSC-EVs promote the differentiation of Tregs in asthmatic patients by transferring miR-1470,[42] prevent group 2 innate lymphoid cell-dominant allergic airway inflammation through delivery of miR-146a-5p,[43] and reduce bronchial smooth muscle cell proliferation via miRNA-188.[44] In fact, EVs can regulate the functional properties of specific cells by transferring miRNAs and/or delivering bioactive proteins.[45] Nevertheless, whether MSC-EVs can affect target cell function by transferring proteins under asthmatic conditions remains unknown. In this study, we first screened Hypo-EVs for several known cytoprotective proteins in airway epithelial cells in asthma and found that CAV-1 was the most abundant. As a major component of caveolae, CAV-1 is highly conserved in mammals, and consistent with previous reports,[46,47] we found that CAV-1 protein expression was lower in airway epithelia of asthma animal models. Combined with the following evidences: (1) Hypo-EVs can be taken up by BEC cells in vivo and in vitro; (2) Hypo-EV treatment significantly increased the protein levels of CAV-1 in asthma mice or type-2 cytokines-induced BEC; (3) CAV-1 can be transferred into BEC cells through Hypo-EVs; (4) Hypo-EVs with CAV-1 knockdown impaired the barrier-protection effects of Hypo-EVs on BEC cells in vitro and asthma mice in vivo, we concluded that nebulization of Hypo-EVs attenuate airway epithelial barrier defects in chronic asthma mice by transferring CAV-1. Furthermore, we found that CAV-1 knockdown impaired the improvement effect of Hypo-EVs on airway inflammation and airway remodeling in mice with chronic asthma, which not only confirmed the lung-protective function of aerosolized Hypo-EVs in asthma but also highlighted CAV-1 as a potential biofactor for alleviating chronic inflammatory respiratory diseases.[47] However, our present results cannot exclude the possibility that other proteins in Hypo-EVs may also play a role. In addition, because MSC-EVs are versatile drug delivery platforms,[48] engineering MSC-EVs using bioactive proteins that have lung-protective effects might also be a promising option for asthma intervention, and more evidence is needed to address this concern.

A recent study reported that STAT6 signaling is necessary for IL-4/IL-13-induced decrease in ZO-1 expression in airway epithelial cells.[49] In this study, we found that except for ZO-1, the downregulation of E-cadherin in response to IL-4/IL-13 was reversed after using the selective STAT6 inhibitor AS1517499. In addition, we showed that the permeability of epithelial cells, induced by IL-4/IL-13, was reduced by AS1517499 treatment. These findings demonstrated that the STAT6 pathway, which is commonly activated in lung injury (eg, asthma[50]), may be critical in the modulation of type type-2 cytokines-induced airway epithelial barrier defects.

We further explored the underlying mechanisms by which Hypo-EV-derived CAV-1 exerts barrier-protective effects. CAV-1 has been confirmed to be a vital factor in the regulation of signal transduction, such as the inhibition of transforming growth factor (TGF)-beta/SMAD signaling,[37] regulation of the STAT3 pathway,[51,52] activation of Rho-associated coiled-coil kinase-1,[53] and downregulating NF-κB pathway[54] and so on. However, it is not clear whether CAV-1 regulates STAT6 signaling. In this study, we found that CAV-1 significantly reduced the levels of p-STAT6 in IL-4/IL-13-induced BEC, accompanied by the upregulation of ZO-1 and E-cadherin. These results not only indicated that CAV-1 could inhibit p-STAT6, but also emphasized that CAV-1 is upstream of ZO-1 and E-cadherin. Then, we examined the p-STAT6 expression in IL-4/IL-13-induced BEC cells in vitro and in asthma mice lung, and found that p-STAT6 levels were decreased by Hypo-EV treatment, more importantly, compared with EVs-NC group, EVs-KD significantly increased the protein levels of p-STAT6. Therefore, we postulated that Hypo-EV-derived CAV-1 may protect the airway barrier by inhibiting p-STAT6, which is involved in ZO-1 and E-cadherin upregulation. However, the mechanism by which CAV-1 regulates STAT 6 signal remains unclear. Furthermore, we do not exclude that Hypo-EVs may inhibit p-STAT6 expression by delivering other active substances, which needs to be demonstrated in the future. In addition, we speculated that IL-4/IL-13 might be a negative regulator of CAV-1 expression in the lung because IL-4/IL-13 can markedly decrease the expression of CAV-1 in BEC cells, as shown in this study.

This study had some limitations. First, OVA-induced asthmatic mice and the corresponding IL-4/IL-13-induced airway epithelial barrier dysfunction model were used, which has been widely used in many studies. However, house dust mite (HDM) models show a closer resemblance to human asthma, and HDM could directly cleave airway epithelial junctions proteolytically.[6] Therefore, the inhibitory effects of MSC-EVs need to be tested on those asthma models. On the other hand, due to the current unavailability of the relevant equipment in our laboratory, transepithelial electrical resistance, an important parameter for assessing the integrity of the airway epithelial barrier, were not detected. Third, we only used a single dosage of Hypo-EVs in our experiments. Further studies are required to determine the dose-dependent responses to find the most effective doses while considering the potential for cytotoxicity.

Conclusion

In summary, our study is the first to confirm the therapeutic efficacy of Hypo-EVs in airway epithelial barrier defects under asthmatic conditions in vivo and in vitro. This may be mediated by the delivery of CAV-1 to bronchial epithelial cells to inhibit the p-STAT6 pathways, thus enhancing ZO-1 and E-cadherin expression. These findings provide different mechanisms for understanding the lung-protective effect of MSC-EVs against asthma and suggest that nebulization of Hypo-EVs might also be appropriate for treating other airway leakage-related diseases, such as chronic rhinitis and COPD.

Abbreviations

MSCs, mesenchymal stem cells; hUCMSCs, human umbilical cord MSCs; EVs, extracellular vesicles; Hypo-EVs, hypoxic hUCMSC-derived EVs; BEC, bronchial epithelial cells; HSP70, heat shock protein 70; TSG101, tumor susceptibility gene 101; PBS, phosphate-buffered saline; HE, hematoxylin and eosin; Masson, Masson trichrome staining; OVA, ovalbumin; PAS, periodic acid–Schiff; BALF, bronchoalveolar lavage fluid; IL, interleukin; WB, Western blotting; NTA, nanoparticle trafficking analysis; TEM, transmission electron microscope; CAV-1, caveolin-1; STAT6, signal transducer and activator of transcription 6; HRP, horseradish Peroxidase; ELISA, enzyme-linked immune sorbent assay; EpCAM, epithelial cell adhesion molecule; CCK-8, Cell Counting Kit-8; FITC, Fluorescein isothiocyanate; DEX, dextran; Papp, apparent permeability coefficient; ERBB2, erythroblastosis oncogene B2; ITGB4, integrin β4;

NRF2, Nuclear erythroid 2-related factor 2; siRNA, small interfering RNA; NC, negative control; KD, knockdown; SD, standard deviation; TGF-β, transforming growth factor beta; NF-κB, nuclear factor kappa-B; HDM, house dust mite; COPD, chronic obstructive pulmonary diseases.

Data Sharing Statement

Data supporting the findings of this study are available from the corresponding author upon reasonable request.

Ethic Approval and Informed Consent

Human umbilical cord samples were obtained from mothers who provided informed consent at the Affiliated Hospital of Jiangsu University, which abides by the Helsinki Declaration on ethical principles for medical research involving human participants. This study was approved by the Ethics Committee of the Affiliated Hospital of Jiangsu University (no. SWYXLL20200121-22). All animal experiments were approved by the Institutional Animal Care and Use Committee of Jiangsu University (No. UJS-IACUC-AP-2023050902). Animal welfare was ensured in accordance with the Guide for the Care and Use of Laboratory Animals.

Funding

This work was supported by grants from the National Natural Science Foundation of China (82300035; 81900562), Medical Research Project of Jiangsu Provincial Health Commission (H2023021), and "XueDiJiFang" Projects of Jiangsu Province (x202306).

Disclosure

The authors declare no potential conflicts of interest in this work.

References

1. Hay S. Global, regional, and national deaths, prevalence, disability-adjusted life years, and years lived with disability for chronic obstructive pulmonary disease and asthma, 1990–2015: a systematic analysis for the Global Burden of Disease Study 2015. *Lancet Respir Med*. 2017;5(9):691–706. doi:10.1016/s2213-2600(17)30293-x
2. Papi A, Brightling C, Pedersen SE, Reddel HK. Asthma. *Lancet*. 2018;391(10122):783–800. doi:10.1016/s0140-6736(17)33311-1
3. King-Biggs MB. Asthma. *Ann Intern Med*. 2019;171(7):Itc49–itc64. doi:10.7326/aitc201910010
4. Wener RR, Bel EH. Severe refractory asthma: an update. *Eur Respir Rev*. 2013;22(129):227–235. doi:10.1183/09059180.00001913
5. Russell RJ, Boulet LP, Brightling CE, et al. The airway epithelium: an orchestrator of inflammation, a key structural barrier and a therapeutic target in severe asthma. *Eur Respir J*. 2024;63(4). doi:10.1183/13993003.01397-2023
6. Heijink IH, Kuchibhotla VNS, Roffel MP, et al. Epithelial cell dysfunction, a major driver of asthma development. *Allergy*. 2020;75(8):1902–1917. doi:10.1111/all.14421
7. Hellings PW, Steelant B. Epithelial barriers in allergy and asthma. *J Allergy Clin Immunol*. 2020;145(6):1499–1509. doi:10.1016/j.jaci.2020.04.010
8. Wawrzyniak P, Wawrzyniak M, Wanke K, et al. Regulation of bronchial epithelial barrier integrity by type 2 cytokines and histone deacetylases in asthmatic patients. *J Allergy Clin Immunol*. 2017;139(1):93–103. doi:10.1016/j.jaci.2016.03.050
9. Komlósi ZI, van de Veen W, Kovács N, et al. Cellular and molecular mechanisms of allergic asthma. *Mol Aspects Med*. 2022;85:100995. doi:10.1016/j.mam.2021.100995
10. Dong X, Ding M, Zhang J, et al. Involvement and therapeutic implications of airway epithelial barrier dysfunction in type 2 inflammation of asthma. *Chin Med J*. 2022;135(5):519–531. doi:10.1097/cm9.0000000000001983
11. Ding JY, Chen MJ, Wu LF, et al. Mesenchymal stem cell-derived extracellular vesicles in skin wound healing: roles, opportunities and challenges. *Mil Med Res*. 2023;10(1):36. doi:10.1186/s40779-023-00472-w
12. Lotfy A, AboQuella NM, Wang H. Mesenchymal stromal/stem cell (MSC)-derived exosomes in clinical trials. *Stem Cell Res Ther*. 2023;14(1):66. doi:10.1186/s13287-023-03287-7
13. Abbaszadeh H, Ghorbani F, Abbaspour-Aghdam S, et al. Chronic obstructive pulmonary disease and asthma: mesenchymal stem cells and their extracellular vesicles as potential therapeutic tools. *Stem Cell Res Ther*. 2022;13(1):262. doi:10.1186/s13287-022-02938-5
14. Dong L, Wang Y, Zheng T, et al. Hypoxic hUCMSC-derived extracellular vesicles attenuate allergic airway inflammation and airway remodeling in chronic asthma mice. *Stem Cell Res Ther*. 2021;12(1):4. doi:10.1186/s13287-020-02072-0
15. Xu X, Wang Y, Luo X, et al. A non-invasive strategy for suppressing asthmatic airway inflammation and remodeling: inhalation of nebulized hypoxic hUCMSC-derived extracellular vesicles. *Front Immunol*. 2023;14:1150971. doi:10.3389/fimmu.2023.1150971
16. Dong L, Pu Y, Zhang L, et al. Human umbilical cord mesenchymal stem cell-derived extracellular vesicles promote lung adenocarcinoma growth by transferring miR-410. *Cell Death Dis*. 2018;9(2):218. doi:10.1038/s41419-018-0323-5
17. Cho KS, Park MK, Kang SA, et al. Adipose-derived stem cells ameliorate allergic airway inflammation by inducing regulatory T cells in a mouse model of asthma. *Mediators Inflamm*. 2014;2014:436476. doi:10.1155/2014/436476

18. Padrid P, Snook S, Finucane T, et al. Persistent airway hyperresponsiveness and histologic alterations after chronic antigen challenge in cats. *Am J Respir Crit Care Med*. 1995;151(1):184–193. doi:10.1164/ajrccm.151.1.7812551
19. de Castro LL, Xisto DG, Kitoko JZ, et al. Human adipose tissue mesenchymal stromal cells and their extracellular vesicles act differentially on lung mechanics and inflammation in experimental allergic asthma. *Stem Cell Res Ther*. 2017;8(1):151. doi:10.1186/s13287-017-0600-8
20. Zhang W, Li L, Zheng Y, et al. Schistosoma japonicum peptide SJMHE1 suppresses airway inflammation of allergic asthma in mice. *J Cell Mol Med*. 2019;23(11):7819–7829. doi:10.1111/jcmm.14661
21. Dong L, Pu Y, Chen X, et al. hUCMSC-extracellular vesicles downregulated hepatic stellate cell activation and reduced liver injury in S. japonicum-infected mice. *Stem Cell Res Ther*. 2020;11(1):21. doi:10.1186/s13287-019-1539-8
22. Smyth T, Veazey J, Eliseeva S, Chalupa D, Elder A, Georas SN. Diesel exhaust particle exposure reduces expression of the epithelial tight junction protein Tricellulin. *Part Fibre Toxicol*. 2020;17(1):52. doi:10.1186/s12989-020-00383-x
23. Xu S, Xue X, You K, Fu J. Caveolin-1 regulates the expression of tight junction proteins during hyperoxia-induced pulmonary epithelial barrier breakdown. *Respir Res*. 2016;17(1):50. doi:10.1186/s12931-016-0364-1
24. Shintani Y, Maruoka S, Gon Y, et al. Nuclear factor erythroid 2-related factor 2 (Nrf2) regulates airway epithelial barrier integrity. *Allergol Int*. 2015;64:S54–S63. doi:10.1016/j.alit.2015.06.004
25. Dong L, Ding C, Zheng T, et al. Extracellular vesicles from human umbilical cord mesenchymal stem cells treated with siRNA against ELFN1-AS1 suppress colon adenocarcinoma proliferation and migration. *Am J Transl Res*. 2019;11(11):6989–6999.
26. Dong L, Wang X, Tan J, et al. Decreased expression of microRNA-21 correlates with the imbalance of Th17 and Treg cells in patients with rheumatoid arthritis. *J Cell Mol Med*. 2014;18(11):2213–2224. doi:10.1111/jcmm.12353
27. Bandeira E, Oliveira H, Silva JD, et al. Therapeutic effects of adipose-tissue-derived mesenchymal stromal cells and their extracellular vesicles in experimental silicosis. *Respir Res*. 2018;19(1):104. doi:10.1186/s12931-018-0802-3
28. Zhao H, Peng H, Cai SX, Li W, Zou F, Tong W. Toluene diisocyanate enhances human bronchial epithelial cells' permeability partly through the vascular endothelial growth factor pathway. *Clin Exp Allergy*. 2009;39(10):1532–1539. doi:10.1111/j.1365-2222.2009.03300.x
29. Lu X, Jiang G, Gao Y, et al. Platelet-derived extracellular vesicles aggravate septic acute kidney injury via delivering ARF6. *Int J Biol Sci*. 2023;19(16):5055–5073. doi:10.7150/ijbs.87165
30. Hu Y, Zhang Y, Ni CY, et al. Human umbilical cord mesenchymal stromal cells-derived extracellular vesicles exert potent bone protective effects by CLEC11A-mediated regulation of bone metabolism. *Theranostics*. 2020;10(5):2293–2308. doi:10.7150/thno.39238
31. Inoue H, Hattori T, Zhou X, et al. Dysfunctional ErbB2, an EGF receptor family member, hinders repair of airway epithelial cells from asthmatic patients. *J Allergy Clin Immunol*. 2019;143(6):2075–2085.e10. doi:10.1016/j.jaci.2018.11.046
32. Yuan L, Liu H, Du X, et al. Airway epithelial ITGB4 deficiency induces airway remodeling in a mouse model. *J Allergy Clin Immunol*. 2023;151(2):431–446.e16. doi:10.1016/j.jaci.2022.09.032
33. Hackett TL, de Bruin HG, Shaheen F, et al. Caveolin-1 controls airway epithelial barrier function. Implications for asthma. *Am J Respir Cell Mol Biol*. 2013;49(4):662–671. doi:10.1165/rcmb.2013-0124OC
34. Sweerus K, Lachowicz-Scroggins M, Gordon E, et al. Claudin-18 deficiency is associated with airway epithelial barrier dysfunction and asthma. *J Allergy Clin Immunol*. 2017;139(1):72–81.e1. doi:10.1016/j.jaci.2016.02.035
35. Sussan TE, Gajghate S, Chatterjee S, et al. Nrf2 reduces allergic asthma in mice through enhanced airway epithelial cytoprotective function. *Am J Physiol Lung Cell Mol Physiol*. 2015;309(1):L27–L36. doi:10.1152/ajplung.00398.2014
36. Jia M, Yan X, Jiang X, et al. Ezrin, a Membrane Cytoskeleton Cross-Linker Protein, as a Marker of Epithelial Damage in Asthma. *Am J Respir Crit Care Med*. 2019;199(4):496–507. doi:10.1164/rccm.201802-0373OC
37. Gandhi NA, Bennett BL, Graham NM, Pirozzi G, Stahl N, Yancopoulos GD. Targeting key proximal drivers of type 2 inflammation in disease. *Nat Rev Drug Discov*. 2016;15(1):35–50. doi:10.1038/nrd4624
38. Zhang GY, Yu Q, Cheng T, et al. Role of caveolin-1 in the pathogenesis of tissue fibrosis by keloid-derived fibroblasts in vitro. *Br J Dermatol*. 2011;164(3):623–627. doi:10.1111/j.1365-2133.2010.10111.x
39. Hamid Q, Tulic M. Immunobiology of asthma. *Annu Rev Physiol*. 2009;71:489–507. doi:10.1146/annurev.physiol.010908.163200
40. Li J, Sun S, Zhu D, et al. Inhalable Stem Cell Exosomes Promote Heart Repair After Myocardial Infarction. *Circulation*. 2024;150(9):710–723. doi:10.1161/circulationaha.123.065005
41. Qiu W, Guo Q, Guo X, et al. Mesenchymal stem cells, as glioma exosomal immunosuppressive signal multipliers, enhance MDSCs immunosuppressive activity through the miR-21/SP1/DNMT1 positive feedback loop. *J Nanobiotechnology*. 2023;21(1):233. doi:10.1186/s12951-023-01997-x
42. Zhuansun Y, Du Y, Huang F, et al. MSCs exosomal miR-1470 promotes the differentiation of CD4(+)CD25(+)FOXP3(+) Tregs in asthmatic patients by inducing the expression of P27KIP1. *Int Immunopharmacol*. 2019;77:105981. doi:10.1016/j.intimp.2019.105981
43. Fang SB, Zhang HY, Wang C, et al. Small extracellular vesicles derived from human mesenchymal stromal cells prevent group 2 innate lymphoid cell-dominant allergic airway inflammation through delivery of miR-146a-5p. *J Extracell Vesicles*. 2020;9(1):1723260. doi:10.1080/20013078.2020.1723260
44. Shan L, Liu S, Zhang Q, Zhou Q, Shang Y. Human bone marrow-mesenchymal stem cell-derived exosomal microRNA-188 reduces bronchial smooth muscle cell proliferation in asthma through suppressing the JARID2/Wnt/β-catenin axis. *Cell Cycle*. 2022;21(4):352–367. doi:10.1080/15384101.2021.2020432
45. Mathieu M, Martin-Jaular L, Lavieu G, Théry C. Specificities of secretion and uptake of exosomes and other extracellular vesicles for cell-to-cell communication. *Nat Cell Biol*. 2019;21(1):9–17. doi:10.1038/s41556-018-0250-9
46. Bains SN, Tourkina E, Atkinson C, et al. Loss of caveolin-1 from bronchial epithelial cells and monocytes in human subjects with asthma. *Allergy*. 2012;67(12):1601–1604. doi:10.1111/all.12021
47. Royce SG, Le Saux CJ. Role of caveolin-1 in asthma and chronic inflammatory respiratory diseases. *Expert Rev Respir Med*. 2014;8(3):339–347. doi:10.1586/17476348.2014.905915
48. Sun Y, Liu G, Zhang K, Cao Q, Liu T, Li J. Mesenchymal stem cells-derived exosomes for drug delivery. *Stem Cell Res Ther*. 2021;12(1):561. doi:10.1186/s13287-021-02629-7
49. Moonwiriyakit A, Yimnual C, Noitem R, et al. GPR120/FFAR4 stimulation attenuates airway remodeling and suppresses IL-4- and IL-13-induced airway epithelial injury via inhibition of STAT6 and Akt. *Biomed Pharmacother*. 2023;168:115774. doi:10.1016/j.biopha.2023.115774
50. Walford HH, Doherty TA. STAT6 and lung inflammation. *Jak-stat*. 2013;2(4):e25301. doi:10.4161/jkst.25301

51. Kunzmann S, Collins JJ, Yang Y, et al. Antenatal inflammation reduces expression of caveolin-1 and influences multiple signaling pathways in preterm fetal lungs. *Am J Respir Cell Mol Biol*. 2011;45(5):969–976. doi:10.1165/rcmb.2010-0519OC
52. Tong F, Shen W, Zhao J, et al. Silencing information regulator 1 ameliorates lipopolysaccharide-induced acute lung injury in rats via the upregulation of caveolin-1. *Biomed Pharmacother*. 2023;165:115018. doi:10.1016/j.biopha.2023.115018
53. Liu Y, Fu Y, Hu X, et al. Caveolin-1 knockdown increases the therapeutic sensitivity of lung cancer to cisplatin-induced apoptosis by repressing Parkin-related mitophagy and activating the ROCK1 pathway. *J Cell Physiol*. 2020;235(2):1197–1208. doi:10.1002/jcp.29033
54. He R, Yuan X, Lv X, Liu Q, Tao L, Meng J. Caveolin-1 negatively regulates inflammation and fibrosis in silicosis. *J Cell Mol Med*. 2022;26(1):99–107. doi:10.1111/jcmm.17045